OSIRIS: A SIMULATOR OF OUTDOOR SCENES IN THERMAL INFRARED RANGE

T. Poglio [a,b] *, E. Savaria [a], L. Wald [b]

[a] Alcatel Space Industries, System Architecture Division, 06156 Cannes, France –
(thierry.poglio, eric.savaria)@space.alcatel.fr
[b] Groupe Télédétection & Modélisation, Ecole des Mines de Paris, 06904 Sophia Antipolis, France –
(thierry.poglio, lucien.wald)@ensmp.fr

ABSTRACT:

This paper deals with the simulation of very high spatial resolution images in the thermal infrared range, from 3 to 14 µm. It recalls the physical processes occurring in this spectral range. The complexity of the simulation of such processes is explained. The specifications of the simulator and a methodology for the simulation of infrared imagery are proposed. This methodology enables a very accurate simulation of the signal coming from each object constituting the landscape. The interactions between the radiations and objects and the convective and conductive interactions between objects themselves are considered. Their variations in time, and the recent past of the temperature and the humidity for each object, are taken into account. To reproduce these physical phenomena, the computation is performed on elements, which are defined as homogeneous entities with respect to the physical processes. The architecture of the simulator *OSIRIS* using the elements is presented. Finally, examples are shown, showing the efficiency of the simulator and the methodology used.

1. INTRODUCTION

There is a growing concern of very high spatial resolution imagery in the infrared range from 3 to 14 µm. Simulators of landscapes in thermal infrared range need to be developed. One of the major points in the simulation is the accurate knowledge of the input parameters, and particularly the accurate knowledge of the scene to be observed. Synthesis approaches to outdoor scenes offer the possibilities to simulate changing meteorological conditions, different places, different landscapes, different times and different spectral bands.

As physical processes play an essential part in the signal coming from the scene, there is a need for research on spatial, spectral and temporal properties of natural and human-formed objects, their image signatures and their modelling. The synthesis of outdoor scenes in the infrared range is at the crossings of computer vision, physics and remote sensing.

In thermal infrared, the flux coming from an object is partly emitted by the object because of its own temperature, and partly due to the reflection of incident rays on the surface of this object. Depending on the surface material and the spectral band, emission or reflection process dominates the signal. For each object in the scene, the landscape simulator predicts the heat exchanges between objects, the temporal evolution of heat balance, the surface temperature, the spectral emission and the spectral reflection of all incident fluxes. Such a simulator takes into account 3-D landscape description, environmental conditions, thermal and optical characteristics of the objects, and the spectral band of the sensor.

Jaloustre-Audouin (1998) and Jaloustre-Audouin *et al.* (1997) have developed a simulator of any type of landscape in 2-D in the infrared band. Image simulators taking into account a 3-D representation of the landscape as input exist, but they are for visible range or dedicated to specific applications. For example, Thirion (1991) has developed a simulator of high spatial resolution image in the visible range. Johnson *et al.* (1998) have developed a simulator in the infrared range to simulate the behaviour of vehicles. Guillevic (1999) was interested in radiative budget modelling for vegetation canopy studies. Barillot (2001) has developed MISTRAL, which can simulate an image taking into account a 3-D description of the landscape. A simulator of landscape adapted to remote sensing applications does not exist and has to be developed. It should take into account a 3-D description of the scene with high spatial resolution.

Physical processes occurring in the signal coming from the scene are described in the following section. Next, the specifications of the simulator are given. The main difficulties, related to these specifications and the infrared range are explained. A new methodology is proposed for the simulation of very high-resolution 3-D scenes and the consequences on the landscape modelling are explained. Section 4 details the architecture of the simulator using this modelling; each subpart of the simulator is presented, and its operation is explained. Finally, section 5 presents examples of synthesised scenes.

2. PHYSICAL PROCESSES OCCURRING IN THE INFRARED RANGE

2.1 The radiance balance equation

In the general case, the energy equilibrium for a set of radiating objects is expressed, independently on the wavelength l, by the following equation:

---

* Corresponding author.

$$L(x,\boldsymbol{q}_v\boldsymbol{j}_v) = L_e(x,\boldsymbol{q}_v\boldsymbol{j}_v)$$
$$+ \int_{\Omega} f_r(x,\boldsymbol{q}\boldsymbol{j},\boldsymbol{q}_v\boldsymbol{j}_v)L_j(x,\boldsymbol{q}\boldsymbol{j})\cos\boldsymbol{q}d\boldsymbol{w} \qquad (1)$$

Notations and definitions used here are those given by Sillion and Puech (1994). Additional information on transfer in global illumination can be found in Arvo (1993).

- $L(x,\boldsymbol{q}\boldsymbol{j})$, $L_e(x,\boldsymbol{q}_v\boldsymbol{j}_v)$ and $L_j(x,\boldsymbol{q}\boldsymbol{j})$ are respectively the radiance leaving point x in the viewing direction $(\boldsymbol{q}_v\boldsymbol{j}_v)$, the emitted radiance by point x in the same direction, and the incident radiance impinging the point x from direction $(\boldsymbol{q}\boldsymbol{j})$.
- Ω is the set of directions $(\boldsymbol{q}\boldsymbol{j})$ in the hemisphere covering the surface at point x.
- $f_r(x,\boldsymbol{q}\boldsymbol{j},\boldsymbol{q}_v\boldsymbol{j}_v)$ is the bidirectional reflectance distribution function (BDRF) describing the reflective properties of point x (Nicodemus *et al.*, 1977).

Both emitted and incident radiance, the BRDF, and the response g of the instrument depend on the wavelength $\boldsymbol{l}$.

BRDF models exist in the visible range (Rusinkiewicz, 1997). They usually depend on about five parameters that can be found in databases such as Columbia-Utrecht (2001). Both models and databases are nor assessed in the infrared range. For the sake of concision, we assume lambertian reflectors and emitters, and the isotropy of the BRDF. Considering fluxes G, E, and B_j instead of radiance L, L_e and L_j, and expressing the environment of the object i, the previous equation becomes:

$$G_{i,I_1,I_2} = \int_{I_1}^{I_2} g(\boldsymbol{l})E_i(\boldsymbol{l})d\boldsymbol{l} + \sum_{j=1}^{N} F_{ij}\int_{I_1}^{I_2} g(\boldsymbol{l})r_i(\boldsymbol{l})B_j(\boldsymbol{l})d\boldsymbol{l} \qquad (2)$$

F_{ij} is the form-factor and represents the rate of energy exchange between object i and object j. It can be computed (Schröder *et al.*, 1993) or estimated (Wallace *et al.*, 1989). Due to spectral quantities and integral equations, the radiosity method (Foley, 1996; Watt, 2000) cannot be used easily, except in considering many systems of equations: one system per spectral sample in a given spectral range. Nevertheless, under useful simulation conditions, the number of neighbours N is generally small as well as the form-factor. The previous equation is solved with an iterative method, considering emission and reflection at order k. Equation (2) will be used to compute spectral radiance leaving objects. Radiosity method can be applied when equation (2) is integrated from zero to infinity, to compute energy flux balance impinging objects.

2.2 The prediction of emitted flux and of the temperature

The main difficulty related to equation (2) is to compute the E_i terms that correspond to the self-emission of the object. They can be expressed as the product of the emissivity $\boldsymbol{e}_s$ of the object by the blackbody function L^{bb} at temperature T_s. For lambertian emitters, it comes:

$$E_i(\boldsymbol{l}) = \boldsymbol{p}\cdot\boldsymbol{e}_s(\boldsymbol{l})L^{bb}(T_s,\boldsymbol{l}) \qquad (3)$$

The surface temperature of the object has to be known to make the simulation. This temperature is governed by the heat equation, which can be written under thermodynamical conditions usually encountered in landscapes:

$$\frac{\partial T}{\partial t} = \boldsymbol{k}\cdot\Delta T \qquad (4)$$

where $\boldsymbol{k}$ is the thermal diffusivity, and Δ is the Laplacian operator. This equation may be solved using *e.g.* the finite difference method or the method proposed by Deardorff (1978). Because of thermal inertial, the knowledge of this temperature at t requests the temperature at the previous moment (t-dt). The in-depth temperature of the object, and the energy flux balance at the surface of the object are the two boundary conditions required to solve a second-order differential equation. Given an initial state, an iterative process is harnessed to compute surface temperature at the instant of simulation. The interactions between physical parameters, and their variations in time are modelled. Methods exist to compute these interactions and their changes in time (Johnson, 1995; Jaloustre-Audouin *et al.*, 1997). Because it is iterative, and because of the complexity of models used for the energy flux balance determination, this process is by far the more demanding in computation time of all the simulation processes.

3. METHODOLOGY USED FOR THE SYNTHESIS

3.1 Specifications

In the infrared range, the spectral flux coming from an object depends upon the meteorological conditions existing in the scene: surface temperature, air temperature, humidity of the object, humidity of the atmosphere… and the optical properties of the object itself in the considered spectral range. To perform a simulation, four types of inputs are provided to the simulator:

- the 3-D landscape geometrical description. The landscape is expressed as a set of located and oriented objects, having their own surrounding. Each object is made of several facets, each of them made of the same material,
- the set of the conditions of the simulation for the present time and past hours: day, time, place, sky cloudiness…,
- a database of thermal and optical characteristics of all primary materials existing in the landscape (albedo, spectral reflectance (ASTER, 2000), specific heat, thermal conductivity, roughness, leaf area index for vegetation,…),
- the spectral response of the sensor g.

3.2 Main difficulties related to infrared range

In short-wave radiation, computation is made on facets, which are flat external parts of an object. In thermal infrared range, the synthesis process requests that each point of a facet exhibits the same energy flux balance at instant t: this facet is homogeneous with respect to energy flux balance. Considering *e.g.* the shadow variations, this same facet will not be necessary homogeneous at t+dt, and so on. This introduces difficulties to compute temperatures. The smallest entities representing the scene may be considered, voxels for instance. With voxels,

entity is either sunny or shadowed. Problems rise with respect to the number of voxels multiplied by the computation time used for energy flux balance and temperature determination for a voxel. In a similar way, geometrical facets are heterogeneous with respect to boundary conditions existing on these entities; if computed on facet, surface temperature would not be physically relevant.

Taking into account variations in time of all the interactions differentiates the image synthesis in the infrared range from that in the visible domain. The synthesis methods used for the simulation of landscapes for short wavelengths do not need to reproduce the recent past of the landscape as it is observed in real infrared images. The radiosity method can be used in such a case. In the thermal infrared range, it cannot, except for considering the radiosity method for each voxel and each time-step. An entity permitting to compute both temperatures at each instant during the process and the radiance leaving the scene has to be used.

In addition, a 3-D description of the landscape is necessary to perform a simulation with a very high spatial resolution. In this respect, objects forming the landscape interact each other. Realistic image simulation should reproduce these physical interactions between objects (Poglio *et al.*, 2001a). This adds to the complexity of the simulation process.

3.3 The landscape representation

We defined an *element* as an entity that exhibits homogeneous properties with respect to geometrical considerations, material constitution, and the occurring physical phenomena at each instant (Poglio *et al.*, 2001b). To reduce as many as possible the number of elements, and afterward the computation time, element is defined as the largest entity included in a facet.

The element is a part of an object; it is a 3-D entity. Its external surface is flat and oriented. The in-depth constitution of the element is made of one or several layers of primary materials; for instance, a wall can be made of two layers; construction concrete and insulation. The element is homogeneous with boundary conditions, both internal and external. Figure 1 illustrates the element.

To better understand the element, one may consider a facet; this facet is partly shadowed at instant *t*. These portions of the facet are a preliminary set of elements, which will be subsequently subdivided by taking into account other phenomena and other instants.

The mesh supporting objects constituting the landscape is made of the union of elements for the period of simulation of temperature. Figure 2 illustrates the representation of the landscape. The landscape is divided into objects, objects into facets, facets into elements. In each subdivision, properties and characteristics are inherited from the previous hierarchical level and are added to perform an element-based representation of the landscape.
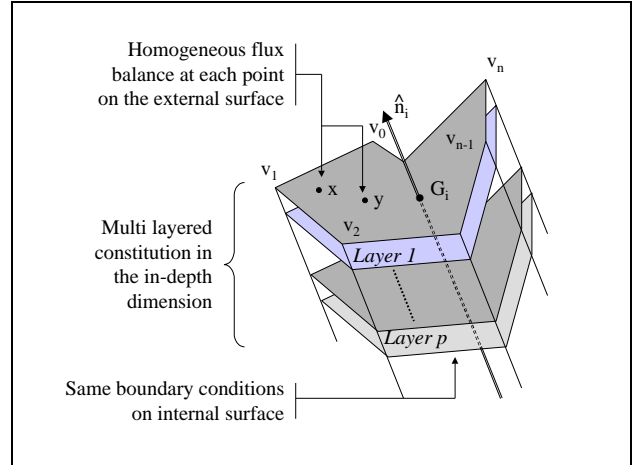

Figure 1: illustration of the multi-layered in-depth constitution of an element and the homogeneity with respect to boundary conditions on both the internal and external surface.
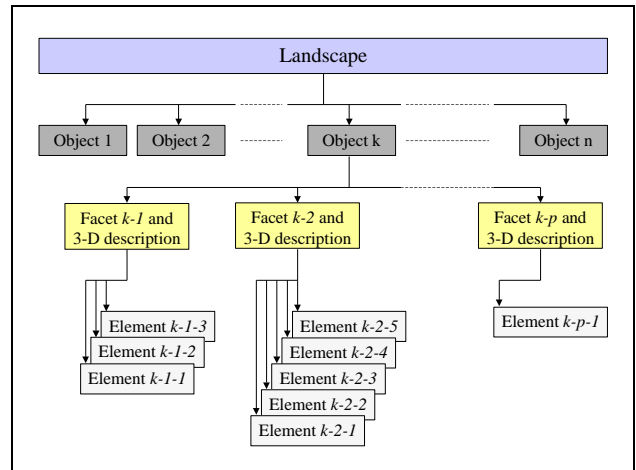

Figure 2: illustration of the landscape element representation.

4. ARCHITECTURE OF THE SIMULATOR *OSIRIS*

The simulator *OSIRIS* is divided into four primary simulators, each of them dealing with a particular sub-part of the simulation (Poglio *et al.*, 2001c). These four primary simulators, called (S0) to (S3), operate successively.

The main technical originality of the simulator *OSIRIS* is the pre-processing simulator, (S0), generating the elements. The simulator (S0) operates with the following scheme (figure 3). The shadow maps are made and combined with the facet description of the scene to obtain the element-based representation. In addition, the radiative and conductive surroundings, the wind velocity for each element and the form-factor matrix are computed.

Figure 3 (flowchart):

Conditions of synthesis — User INPUT | Object-based representation — User INPUT | Materials — User INPUT | Environment rules — User INPUT

Solar flux computation → Temporal sampling

Facet-based modelling → Facet-based representation

Shadow maps computation | Facet heat conduction

Element-based representation

Element visibility computation

Conductive neighbourhood | Radiative neighbourhood

Wind disturbance computation → Wind velocity

Element heat conduction → Conductive neighbourhood

Form-factor computation → Form-factor matrix

Element-based representation
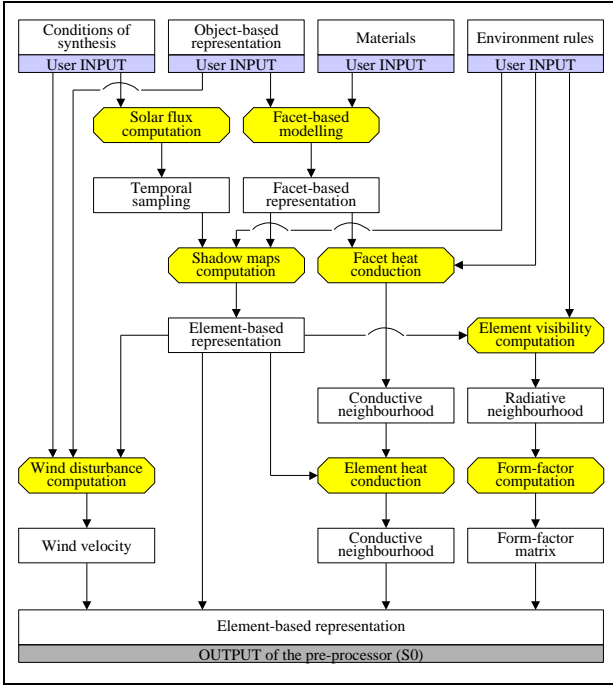
OUTPUT of the pre-processor (S0)

Figure 3: the detailed architecture of the simulator (S0).

All outputs and inputs of (S0) are inputs to (S1). (S1) predicts the surface temperature for each element defined by (S0). The simulator operates in an iterative way. It predicts the heat exchanges, the relative humidity, and the depth-dependent temperature for each element and for each time step (Poglio *et al.*, 2001c). The output of (S1) is the surface temperature for each element constituting the landscape (figure 4).

Figure 4 (flowchart):

Element-based representation — (S0) OUTPUT | In-depth material constitution — User INPUT | Thermal and optical database — DataBase | Conditions of synthesis — User INPUT

Time-step computation

In-depth element mesh computation | Initial state

In-depth element mesh representation | Physical processes modelling (I)

Initialisation | Tabulated values

State of the element at t_0

Differential equation solving for temperature and humidity — While $t \neq t_{simu}$:

State of the element at t | Physical processes modelling (II)

Differential equation solving | Flux balance at t

If $t = t_{simu}$

Element-based representation with temperature and humidity
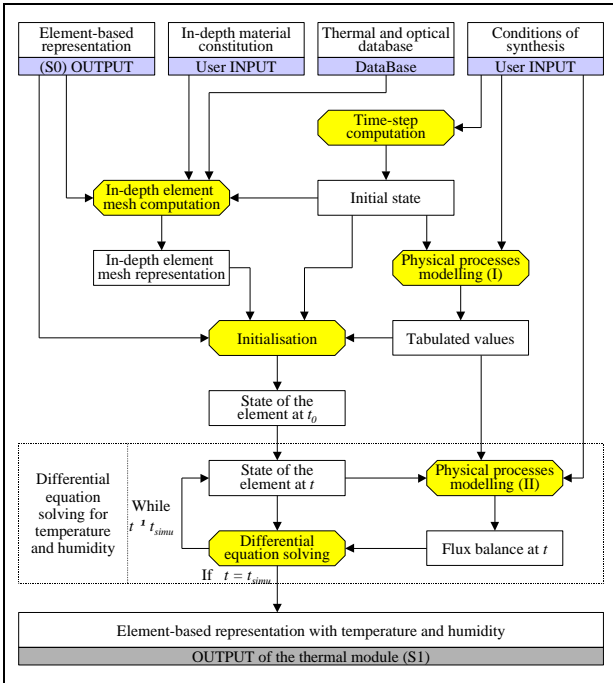
OUTPUT of the thermal module (S1)

Figure 4: the detailed architecture of the simulator (S1).

Then, (S2) simulates spectral emitted and reflected fluxes. Emitted flux is predicted with the help of equation (3) and the (S1) output; ancillary data, like the viewing direction of the scene is required here. Reflected flux computation requires the knowledge of all incident spectral fluxes, especially the sun spectral radiation and the atmospheric spectral radiation (Poglio *et al.*, 2001c). The output of the simulator (S2) is the 3-D scene wherein the emittance of each element is known for the viewing direction (figure 5).

Figure 5 (flowchart):

Temperature representation — (S1) OUTPUT | Spectral database (r, t, e) — DataBase | Conditions of synthesis — User INPUT

Emission computation → Emission for each element

Spectral radiative fluxes computation → Spectral incident fluxes

Reflective fluxes computation → Reflection for each element

Addition of contributions

Global flux (order l)

Iterative computation on the successive orders of reflection:

Global flux (order k) → Iterative computation — While required accuracy not reached

Element-based representation with radiance

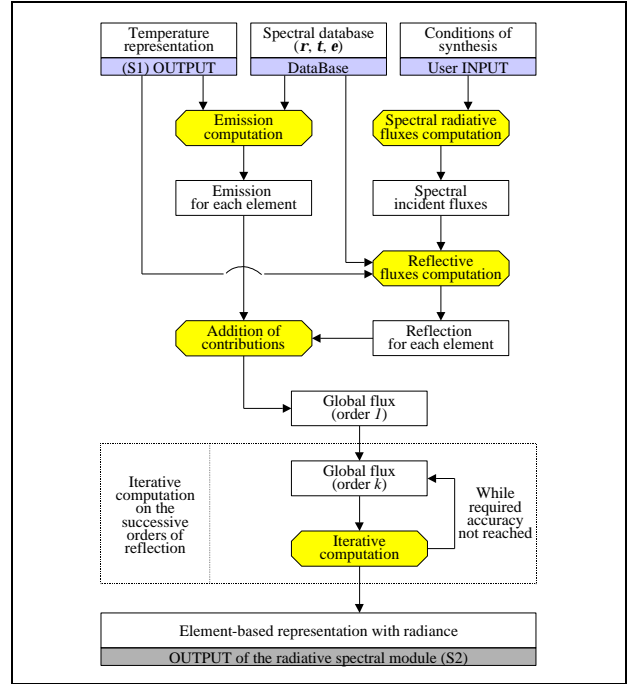OUTPUT of the radiative spectral module (S2)

Figure 5: the detailed architecture of the simulator (S2).

The fourth primary simulator (S3) generates an image for a given viewing angle. Depending on the user preference, this primary simulator generates an image as it would be seen by the sensor, or an image that is only a visualisation of the 3-D scene. The first option requires another simulator to model the acquisition system, such the AS[3]-I simulator of Alcatel Space Industries. The second option offers a visualisation of the 3-D scene. It permits to see the scene without any alteration due to the acquisition system.

The set of these four primary simulators constitutes the simulator *OSIRIS*. The user of such a simulator can be interested in not only the final images, but also in other additional outputs. The element-based representation of the scene, the surface temperature of each element and the emitted flux or the reflected flux for example, are such outputs. They can be used for the training of future users, and to relate each of the inputs and initial conditions to a change in the simulated image.

5. RESULTS AND DISCUSSION

The simulation presented here takes place in Amiens in France (latitude: 49.54 N, longitude: 2.18 E). Houses are made of construction concrete, and an internal thermal insulation made

of polystyrene. The central area is a car park made of asphalt, and the square enclosing this park is a bare soil.

5.1 Spectral band impact

The four following images (figure 6) are simulated the 12th of February, at 2 p.m. after a sunny day, and after shadows have scanned half of the scene. All images are viewed with a zenith angle of 30 °, and an azimuth angle of 60 ° East. Figure 6a represents the surface temperature, ranging from 0 °C in the shadows of the facades to 24 °C for sunlit exterior walls. Figure 6b is an image simulated between 3 and 5 µm. Radiance range from approximately 0.6 to 2.8 W.m^{-2}.sr^{-1}. Solar radiation dominates in the signal in this band; contrast between shadowed and sunlit areas is important.

<table>
<tr><td>(a)</td><td>(b)</td></tr>
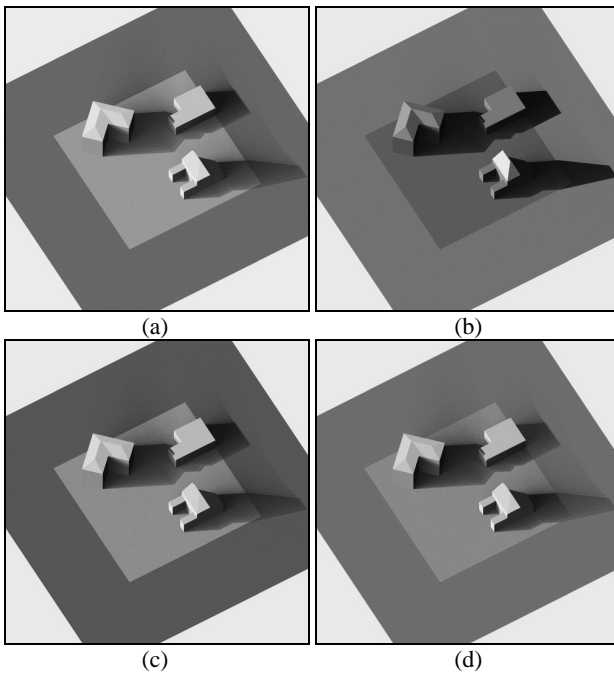<tr><td>(c)</td><td>(d)</td></tr>
</table>

Figure 6: illustration of spectral band impact; (a) image representing surface temperatures, (b), (c) and (d), images in bands 3-5 µm, 8-10 µm and 10-12 µm.

Figures 6c and 6d are images simulated in thermal bands, from 8 to 10 µm and 10 to 12 µm respectively. Influences of the different physical phenomena are approximately the same in these two bands. Radiance range from 12 to 18 W.m^{-2}.sr^{-1}. The difference of contrast between the park made of asphalt and the bare soil is due to the difference of the ratio of emissivity values for those materials in these two bands. It leads to observe a higher contrast from 8 to 10 between the park and the bare soil, and a lower contrast from 10 to 12, compared to temperature image; this is due to self-emission process.

5.2 Temporal shadow effects

The following sequence of images illustrates the shadow variations during the day (figure 7). Images are simulated between 8 and 12 µm, the 21st of June. Not only spatial influence of shadows varies during the day, but also the contrast between shaded and sunlit areas. Another typical effect in the infrared range is the remanence of shadows. Simulations exhibit continuous variations of radiometry in the areas previously

shadowed. This is due to thermal inertia. In the illustration, remanence effect is emphasised on the bare soil, due to the high capacity of this material to store energy.
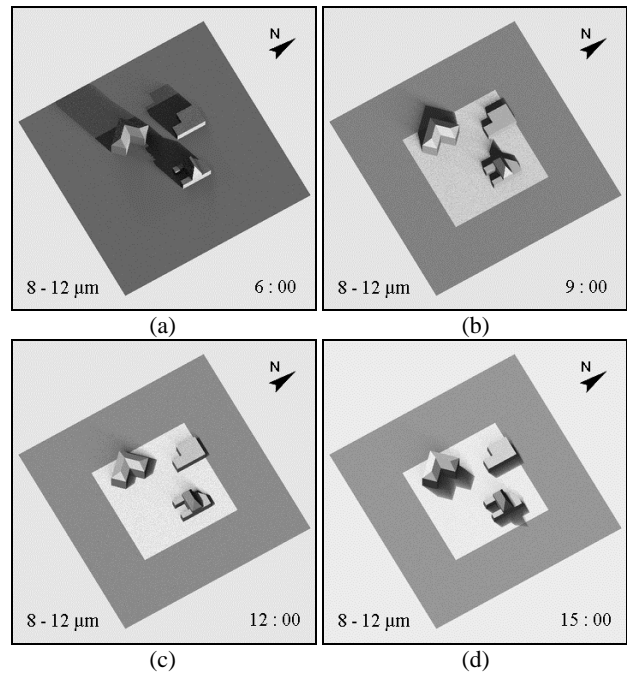

<table>
<tr><td>(a)</td><td>(b)</td></tr>
<tr><td>(c)</td><td>(d)</td></tr>
</table>

Figure 7: illustration of the shadow variations during the day; images are simulated between 8 and 12 µm, at 6 and 9 a.m. and at 12 and 15 p.m.

6. CONCLUSION

The study demonstrates that realistic representation of the landscape is only possible with a 3-D representation, as the sampling rate increases in both time and space. In this respect, objects that form the landscape interact each other. A simulator of realistic images should reproduce faithfully these physical interactions between objects. In the infrared range, the main physical phenomena affecting the signal emitted by the scene are shadow effect, wind disturbance linked to landscape relief, multiple reflections or heat conduction.

The above conclusions were used as a starting point in the specification, the design and the development of a simulator of landscapes in the thermal infrared range with a very high spatial resolution. The physical process underlying the emitted flux in thermal infrared is very complex. The recent history of the landscape is present in the simulated image. The accuracy of the models of the physical processes and their interactions should be high in order to obtain a good quality. Consequently, a new methodology has been devised to design a simulator of landscape described by a 3-D representation.

For an efficient implementation of the 3-D properties, the concept of element was defined. It permits to describe in an accurate manner the objects of the landscape with respect to the physical processes and their variations in time and interactions. The elements are homogeneous entities with respect to geometry, material and temporal evolution of physical phenomena. The architecture of the simulator was adapted to this concept of element and to the specificity of the simulation in the thermal infrared range. The simulator is made of four

primary simulators, each of them having a well-defined role with respect to the description of the landscape on the physical processes.

The present study demonstrates the relevance of such a new methodology. Unavoidably it requests considerable efforts in landscape modelling, software development and computational resources, compared to simulation in the visible range. A first version of this simulator *OSIRIS* was developed as a proof-of-concept. It provides realistic images of outdoor scenes in the infrared range.

REFERENCES

References from Journals:
Deardorff J.W., 1978. Efficient prediction of ground surface temperature and moisture with inclusion of a layer of vegetation. *Journal of Geophysical Research*, **83**, C4, 1889-1902.

Thirion J.-P., 1991. Realistic 3-D simulation of shapes and shadows for image processing. *CVGIP: Graphical Models and Image Processing*, **54** (1), 82-90.

Wallace J.R., Elmquist K.A., Haines E.A., 1989. A ray tracing algorithm for progressive radiosity. *Computer Graphics*, **23** (3), 315-324.

References from Books:
Foley J.D., van Dam A., Feiner S. K., Hughes J. F., 1996. *Computer Graphics, Principles and Practice. Second Edition in C*. Addison-Wesley Publishing Company, ISBN 0-201-84840-b, USA.

Nicodemus F.E., Richmond J.C., Hsia J.J., 1977. Geometrical considerations and nomenclature for reflectance, NBS Monograph 160, U.S. National Bureau of Standards, Washington, D.C.

Sillion F.X., and Puech C., 1994. *Radiosity & Global Illumination*. Morgan Kaufmann Publishers, Inc., ISBN 1-558-60277-1, San Francisco, CA, U.S.A., 251 p.

Watt A., 2000. *3-D Computer Graphics*, Third Edition, Addison-Wesley Publishing Compagny Inc, ISBN 0-201-39855-9.

References from Other Literature:
Arvo J., 1993. Transfer equation in global illumination, *Global illumination*, SIGGRAPH'93 Course Notes, **42**.

Guillevic P., 1999. Modélisation des bilans radiatif et énergétique des couverts végétaux. Thèse de Doctorat, Université P. Sabatier, Toulouse, France, 181 p.

Jaloustre-Audouin K., Savaria E., Wald L., 1997. Simulated images of outdoor scenes in infrared spectral band, AeroSense'97, SPIE, Orlando, USA.

Jaloustre-Audouin K., 1998. SPIRou : Synthèse de Paysage en InfraRouge par modélisation physique des échanges à la surface. Thèse de Doctorat, Université de Nice-Sophia Antipolis, Nice, France, 169 p.

Johnson K., Curran A., Less D., Levanen D., Marttila E., Gonda T., Jones J., 1998. MuSES: A new heat and signature management design tool for virtual prototyping, *In* Proceedings of the 9th Annual Ground Target Modelling & Validation Conference, Houghtoon, MI.

Johnson K.R., Wood S.B., Rynes P.L., Yee B.K., Burroughs F.C., Byrd T.,1995. A methodology for rapid calculation of computational thermal models, SAE International Congress & Exposition, Underhood Thermal Management Session, Detroit, Michigan.

Poglio T., Savaria E., Wald L., 2001a. Influence of the three-dimensional effects on the simulation of landscapes in thermal infrared. Proceedings of the 21st Symposium EARSeL, Marne-la-Vallée, France, 133-139.

Poglio T., Ranchin T., Savaria E., Wald L., 2001b. Simulation d'images dans l'infrarouge thermique par approche synthétique: spécifications et architecture fonctionnelle, Proceedings de la journée thématique "Coopération Analyse d'Images et Modélisation", LIGIM, Université Claude Bernard Lyon I, 58-61.

Poglio T., Savaria E., Wald L., 2001c. Specifications and conceptual architecture of a thermal infrared simulator of landscapes, to appear in the proceedings Sensors, Systems, and Next Generation Satellites VII, 8th International Symposium on Remote Sensing, SPIE, Toulouse, France.

Schröder P., and Hanrahan P., 1993. On the form factor between two polygons. *In* Computer Graphics Proceedings, Annual Conference Series: SIGGRAPH'93 (Anaheim, CA), 163-164. ACM SIGGRAPH, New York.

References from websites:
ASTER, 2000. ASTER spectral library Ver 1.2, CD-ROM, Jet Propulsion Laboratory, NASA, October 2000, http://spectib.jpl.nasa.gov/archive/jhu.html.

Barillot, P., June 2001, MISTRAL, ONERA DOTA, http://www.onera.fr/dota/mistral/index.html.

Columbia-Utrecht, http://www.cs.columbia.edu/CAVE/curet/, 2001.

Rusinkiewicz S., 1997. A survey of BRDF representation for computer graphics, CS348c, 9 p, http://www.cs.princeton.edu/~smr/cs348c-97/.